

Phenomenology of keV sterile neutrino in minimal extended seesaw

Pritam Das

Department of Physics, Tezpur University, Assam - 784 028, India
 pritam@tezu.ernet.in

Mrinal Kumar Das

Department of Physics, Tezpur University, Assam - 784 028, India
 mkdas@tezu.ernet.in

We explore the possibility of a single generation of keV scale sterile neutrino (m_S) as a dark matter candidate within the minimal extended seesaw (MES) framework and its influence in neutrinoless double beta decay ($0\nu\beta\beta$) study. Three hierarchical right-handed neutrinos were considered to explain neutrino mass. We also address baryogenesis via the mechanism of thermal leptogenesis considering the decay of the lightest RH neutrino to a lepton and Higgs doublet. A generic model based on $A_4 \times Z_4 \times Z_3$ flavor symmetry is constructed to explain both normal and inverted hierarchy mass pattern of neutrinos. Significant results on effective neutrino masses are observed in presence of sterile mass (m_S) and active-sterile mixing (θ_S) in $0\nu\beta\beta$. Results from $0\nu\beta\beta$ give stringent upper bounds on the active-sterile mixing matrix element. To establish sterile neutrino as dark matter within this model, we checked decay width and relic abundance of the sterile neutrino, which restricted sterile mass (m_S) within some definite bounds. Constrained regions on the CP-phases and Yukawa couplings are obtained from $0\nu\beta\beta$ and baryogenesis results. Co-relations among these observable are also established and discussed within this framework.

Keywords: Beyond Standard Model, Minimal extended seesaw, Sterile neutrino, dark matter, $0\nu\beta\beta$, baryogenesis, thermal leptogenesis

PACS numbers:

1. INTRODUCTION

The discovery of neutrino mass and the Higgs Boson have brought glory to the field of particle physics as well as to astrophysics and cosmology. Experimental results in the field of neutrinos¹⁻⁷ not only verify the theoretical predictions but also open up a new portal to bring physics to the next level^a. In spite of the glorious successes, many unsettled phenomenons and queries are still around us. Exact nature and absolute mass scale of the neutrinos, matter-antimatter asymmetry of the Universe, presence of extra flavor of neutrinos, Dark Matter, *etc.* are among them.

^aRecent global fit results with 3σ bound and best-fit values of the observed neutrino parameters are given in the tabular form in table 1.

Recent results from several cosmological observations^{8–10} as well as reactor data^{11–13} reveal the fact that heavy flavor of neutrinos do exist in the Universe, and they are known as *sterile neutrino*. Sterile neutrinos are neutral right-handed (RH) fermions, and they are singlets under the SM gauge group. Unlike the active neutrinos, they are infertile, *i.e.*, they do not change flavor; however, they mix up with the active neutrinos. For better understanding of sterile neutrino nature and interactions, one may refer to the well established works in.^{14–18} Despite the fact that, the exact mass scale or numbers of sterile neutrino generations are still unknown, their presence may have a significant contribution to the new physics. The presence of sterile neutrino is strongly motivated and highly influences the current reactor neutrino anomalies. Sterile neutrino with different mass ranges play crucial role in astrophysics,¹⁹ cosmology,^{15,16} collider physics,^{20–22} etc. Similar kind of studies were carried out in other context such as LRSM,^{23,24} extra dimensions,^{25,26} in presence of exotic charged currents²⁷ or in relation with *keV* neutrino dark matter.²⁸

Absolute neutrino mass is yet another unknown to the physics community as oscillation experiments are only sensitive to the mass squared difference (Δm_{ij}^2) and leptonic mixing angles (θ_{ij} , with $i, j = 1, 2, 3$). Apart from the oscillation studies, the kinematic study of reactions involving neutrino (ν) and anti-neutrino ($\bar{\nu}$) can give us information about absolute mass. Considering Majorana nature of particles, Wendell Furry²⁹ studied a kinetic process similar to "double-beta disintegration" without neutrino emission, popularly known as *neutrino-less double beta decay* ($0\nu\beta\beta$).³⁰ In simple word this can be expressed as,

$$(A, Z) \rightarrow (A, Z + 2) + 2e^-.$$

From $0\nu\beta\beta$ integration, if Majorana nature of the neutrino is verified, one can give conclusive remark on absolute neutrino mass. The ($0\nu\beta\beta$) process explicitly violates the lepton number by creating a pair of electron. Discovery of lepton number violation (LNV) process supported by existing theoretical picture and the $0\nu\beta\beta$ scenario allows leptons to take part in the process of matter-antimatter asymmetry of our Universe. Thus the observation of such a process is crucial for demonstrating baryogenesis idea³¹ via lepton number violation. Many works on ($0\nu\beta\beta$) have been done considering the SM neutrinos.^{32–35} Nevertheless, it is now clear that the addition of a new scalar fermion and study its interactions within the SM particles can lead us to a broad range of new physics phenomenology.^{18,36}

Shreds of evidence from various sources,^{37–40} it now confirmed the presence of dark matter (DM) into the picture. To understand DM and their mysterious behaviour, we have to understand what it composed of and how they interact with known particles. Among the choices of being a dark matter candidate, dense baryonic and non-baryonic matters were first proposed, and they are largely disfavoured.^{38,41,42} Modifications to the laws of gravitational⁴³ were also not so impressive to explain DM. Since, no SM particle can be a dark matter candidate,^{44–46} so addition of a new particle to the elementary particle list was the only reasonable choice. In the past years, several particles were proposed as DM candidates in BSM and WIMPs

(weakly interacting massive particles) are the most attractive candidates for dark matter at current scenario. WIMPs do not create problems in structure formation like the SM neutrinos does, due to non-relativistic velocity and higher masses. They take different forms under different scenarios like neutralinos under SUSY,^{47,48} Kaluza-Klein bosons as predicted by models based on extra spatial dimensions^{49,50} and minimal extension of the SM scalar sector consider inert doublet scalar as WIMP DM.^{51–53}

Apart from DM and absolute neutrino mass, the overabundance of baryonic matter over the anti-baryonic matter is also discussed in this work. The baryon asymmetry of the Universe (BAU) ($Y_B \equiv \frac{n_B - n_{\bar{B}}}{s} \sim (8.7 \pm 0.06) \times 10^{-11}$)^{b54} is well explained by baryogenesis.^{55,56} Rich literatures available in^{35,57–64} discussing baryogenesis via the mechanism of thermal leptogenesis. We considered thermal leptogenesis, where the heavy RH neutrinos are hierarchical ($M_{\nu_{R1}} < M_{\nu_{R2,3}}$). As per our preferred choice of mass for lightest RH neutrinos,⁵⁷ we are restricted our study to a single flavor leptogenesis.

Motivated by these studies, we are considering a sterile neutrino flavor with a mass around keV range in minimal extended seesaw (MES),^{18,25,65,66} where an additional fermion singlet (sterile neutrino) is added along with three RH neutrinos. The beauty of MES framework is that it can accommodate sterile neutrino mass ranging from eV to keV . Sterile neutrino with eV as well as keV could be probed in future KATRIN experiment.^{67,68} Moreover, keV sterile neutrino has a potential to affect electron energy spectrum in tritium β -decays.⁶⁹ Typically, sterile neutrinos with mass (0.4-50) keV ⁷⁰ are considered as WIMP particles since they are relatively slow and much heavier compared to the active neutrinos. In fact for successfully observe $0\nu\beta\beta$ the upper bound for sterile neutrino mass should be 18.5 keV .^{36,71} Back in the 90s, Dodelson and Widrow¹⁴ proposed keV sterile neutrino as dark matter candidate produced via oscillation and collision from active neutrinos. Recently from various sources like, in the stacked spectrum of galaxy clusters,⁷² individual spectra of nearby galaxy clusters,^{72,73} Andromeda Galaxy,⁷³ and in the Galactic Center region^{74,75} an unidentified line was reported. The position of the line is $E = 3.55 keV$ with an uncertainty in position $\simeq \pm 0.05 keV$. If the line is interpreted as originating from a two-body decay of a DM particle, then the particle has its mass at about $m_S \simeq 7.1 keV$ and the lifetime $\tau_{DM} \simeq 10^{27.8 \pm 0.3} sec$.⁷³ Hence, choosing a mass range for the keV regime sterile neutrino within (1-18.5) keV and explore new possibilities to explain $0\nu\beta\beta$ within laboratory constraints along with DM signature is quite a good choice. Along with the sterile study, we also try to verify baryogenesis produced via the mechanism of thermal leptogenesis within our model and finally, we try to co-relate all these observable under the same framework.

This work is organized as follows: model building with A_4 flavor symmetry along

^b n_B and $n_{\bar{B}}$ are the baryon and anti-baryon number density respectively. s in the denominator is the entropy of the current Universe.

with $Z_4 \times Z_3$ discrete symmetry is discussed in section 2 for both normal (2.1) and inverted (2.2) mass pattern. Numerical analysis is carried out in section 3 and separate sub-section for $0\nu\beta\beta$ (3.1), dark matter (3.2) and baryogenesis via thermal leptogenesis (3.3) are carried out under the same numerical analysis section in a respective manner. Results of our study are discussed in section 4 and finally we conclude our work in section 5.

Table 1. Recent experiments results for active neutrinos parameters with best-fit and the latest global fit 3σ range.⁷⁶

Parameters	NH (Best fit)	IH (Best fit)
$\Delta m_{21}^2 [10^{-5} eV^2]$	6.93-7.97(7.73)	6.93-7.97(7.73)
$\Delta m_{31}^2 [10^{-3} eV^2]$	2.37-2.63(2.50)	2.33-2.60(2.46)
$\sin^2\theta_{12}/10^{-1}$	2.50-3.54(2.97)	2.50-3.54(2.97)
$\sin^2\theta_{13}/10^{-2}$	1.85-2.46(2.14)	1.86-2.48(2.18)
$\sin^2\theta_{23}/10^{-1}$	3.79-6.16(4.37)	3.83-6.37(5.69)
δ_{13}/π	0-2(1.35)	0-2(1.32)

2. The Model

2.1. Normal Hierarchy:

In neutrino model building phenomenology, symmetries have been playing an important role in describing various phenomenology. Interestingly, discrete symmetries like A_4 with Z_n ($n \geq 2$ is integer) are much popular in recent literature in explaining neutrino mass.^{18,77-79} The discrete flavor symmetry A_4 being the symmetry group of rotation with a tetrahedron invariant with 4 irreducible representation denoted by $\mathbf{1}$, $\mathbf{1}'$, $\mathbf{1}''$ and $\mathbf{3}$. The left-handed (LH) lepton doublet l to transform as A_4 triplet whereas the right-handed (RH) charged leptons (e^c, μ^c, τ^c) transform as $\mathbf{1}, \mathbf{1}''$ and $\mathbf{1}'$ respectively. Apart from the type-I seesaw particle content, few extra flavons are added to construct the model. Two triplets ζ, φ , two singlets ξ and ξ' are added to produce broken flavor symmetry. Besides the SM Higgs H_1 , we also introduce an additional Higgs doublets (H_2),^{80,81} to make the model work. Non-desirable interactions were restricted using extra Z_4 and Z_3 charges to the fields. To accommodate sterile neutrino into the framework, we add a chiral gauge singlet S , which interacts with the RH neutrino ν_{R1} via A_4 singlet ($\mathbf{1}'$) flavon χ to give rise to sterile mixing matrix. We used dimension-5 operators⁸² for Dirac neutrino and charged lepton mass generation. One may notice, terms like $\frac{1}{\Lambda} S^c S \varphi \varphi$ may ruin the current MES scenario, by giving rise to unexpectedly higher mass term for the sterile neutrino.⁶⁵ Those terms are excluded by the Z_3 symmetry.

As per the MES structure, the newly added singlet field S does not interact with the active neutrinos, and they can be explained with the Abelian symmetries. For example, by introducing additional $U(1)'$ charge under which the SM particles and

RH neutrinos are to be neutral. The singlet S on the other hand carries a $U(1)'$ charge Y' and we further introduced a SM singlet χ with hypercharge $-Y'$. Hence those coupling of S with the active neutrinos are still forbidden by the $U(1)'$ symmetry at the renormalizable level.^{18,83,84} The particle content with $A_4 \times Z_4 \times Z_3$ charge assignment under NH are shown in the table 2.

Table 2. Particle content and their charge assignments under $SU(2)$, A_4 and $Z_4 \times Z_3$ groups for NH mode.

Particles	l	e_R	μ_R	τ_R	H_1	H_2	ζ	φ	ξ	ξ'	ν_{R1}	ν_{R2}	ν_{R3}	S	χ
SU(2)	2	1	1	1	2	2	1	1	1	1	1	1	1	1	1
A_4	3	1	1''	1'	1	1	3	3	1	1'	1	1'	1	1''	1'
Z_4	1	1	1	1	1	1	i	1	i	1	-1	1	-i	-1	i
Z_3	1	1	1	1	1	1	1	1	1	1	1	1	1	ω^2	ω

In lepton sector, the leading order invariant Yukawa Lagrangian is given by,

$$\begin{aligned}
 \mathcal{L} = & \frac{y_e}{\Lambda} (\bar{l} H_1 \zeta)_1 e_R + \frac{y_\mu}{\Lambda} (\bar{l} H_1 \zeta)_{1'} \mu_R + \frac{y_\tau}{\Lambda} (\bar{l} H_1 \zeta)_{1''} \tau_R \\
 & + \frac{y_2}{\Lambda} (\bar{l} \tilde{H}_1 \zeta)_1 \nu_{R1} + \frac{y_2}{\Lambda} (\bar{l} \tilde{H}_1 \varphi)_{1'} \nu_{R2} + \frac{y_3}{\Lambda} (\bar{l} \tilde{H}_2 \varphi)_1 \nu_{R3} \\
 & + \frac{1}{2} \lambda_1 \xi \overline{\nu_{R1}^c} \nu_{R1} + \frac{1}{2} \lambda_2 \xi' \overline{\nu_{R2}^c} \nu_{R2} + \frac{1}{2} \lambda_3 \xi \overline{\nu_{R3}^c} \nu_{R3} \\
 & + \frac{1}{2} \rho \chi \overline{S^c} \nu_{R1}.
 \end{aligned} \tag{1}$$

In this Lagrangian, various Yukawa couplings are represented by $y_{\alpha,i}$, λ_i (for $\alpha = e, \mu, \tau$ and $i = 1, 2, 3$) and ρ for respective interactions. Higgs doublets are transformed as $\tilde{H} = i\tau_2 H^*$ (τ_2 is the second Pauli's spin matrix) to keep the Lagrangian gauge invariant and Λ is the cut-off scale of the theory, which is around the GUT scale. The scalar flavons involved in the Lagrangian acquire VEV along $\langle \zeta \rangle = (v, 0, 0)$, $\langle \varphi \rangle = (v, v, v)$, $\langle \xi \rangle = \langle \xi' \rangle = v$ and $\langle \chi \rangle = v_\chi$ by breaking the flavor symmetry, while $\langle H_i \rangle (i = 1, 2)$ get VEV (v_i) by breaking EWSB at electro-weak scale. Following the A_4 product rules and using the above mentioned VEV alignment^c, the Dirac neutrino mass^d, Majorana neutrino mass and the sterile mass matrices are given by,

$$M'_D = \begin{pmatrix} D_1 & D_1 & D_2 \\ 0 & D_1 & D_2 \\ 0 & D_1 & D_2 \end{pmatrix}, \quad M_R = \begin{pmatrix} R_1 & 0 & 0 \\ 0 & R_2 & 0 \\ 0 & 0 & R_3 \end{pmatrix}, \quad M_S = (G \ 0 \ 0). \tag{2}$$

^cThe triplet VEV alignment of the scalars are the solution of the respective scalars at their minimal potential⁶⁶

^d M'_D is the unmodified Dirac neutrino mass matrix which is failed to generate $\theta_{13} \neq 0$. The modified M_D is represented in equation (5)

where, $D_1 = \frac{\langle H_1 \rangle v}{\Lambda} y_2$ and $D_2 = \frac{\langle H_2 \rangle v}{\Lambda} y_3$ ^e. Other elements are defined as $R_1 = \lambda_1 v$, $R_2 = \lambda_2 v$, $R_3 = \lambda_3 v$ and $G = \rho v_\chi$. In order to achieve sterile mass in the keV range, we have considered VEV for the χ flavon lie around TeV scale. A rough estimate of the mass scales of parameters are given as, $\Lambda \simeq 10^{14}$ GeV, $v \simeq 10^{13}$ GeV and $v_\chi \simeq 10$ TeV.

We have used similar approaches from our previous work⁶⁶ to break the trivial $\mu - \tau$ symmetry in the light neutrino mass matrix. We introduced two new $SU(2)$ singlet flavon fields (ζ' and φ') which results the M_P matrix (4) when they couple with the respective RH neutrinos. The active mass matrix gets modify by adding the matrix (4) to the Dirac neutrino mass matrix. This new M_P matrix played a significant role in producing non-zero reactor mixing angle and has potential influence in choosing the octant for θ_{23} .⁶⁶ The Lagrangian that generate the matrix (4) can be written as,

$$\mathcal{L}_{\mathcal{M}_P} = \frac{y_1}{\Lambda} (\bar{l} \tilde{H}_1 \zeta')_1 \nu_{R1} + \frac{y_1}{\Lambda} (\bar{l} \tilde{H}_1 \varphi')_{1''} \nu_{R2} + \frac{y_1}{\Lambda} (\bar{l} \tilde{H}_2 \varphi')_1 \nu_{R3}. \quad (3)$$

New $SU(2)$ singlet flavon fields (ζ' and φ') are considered and supposed to take $A_4 \times Z_4 \times Z_3$ charges as same as ζ and φ respectively. After breaking flavor symmetry they acquire VEV along $\langle \zeta' \rangle = (v_p, 0, 0)$ and $\langle \varphi' \rangle = (0, v_p, 0)$ directions, giving rise to the M_P matrix as,

$$M_P = \begin{pmatrix} 0 & 0 & P \\ 0 & P & 0 \\ P & 0 & 0 \end{pmatrix}, \quad (4)$$

with, $P = \frac{\langle H_i \rangle v}{\Lambda} y_i$ ($i=1$ or 2). Scale of these VEV (v_p) in comparison to earlier flavon's VEV (v) are differ by an order of magnitude ($v > v_p$). Involvement of these new flavons are restricted in the leading order Lagrangian charge lepton mass matrix. Hence, the Dirac neutrino mass matrix, M_D from eq. (2) will take new structure as,

$$M_D = M'_D + M_P = \begin{pmatrix} D_1 & D_1 & D_2 + P \\ 0 & D_1 + P & D_2 \\ P & D_1 & D_2 \end{pmatrix}. \quad (5)$$

2.2. Inverted Hierarchy

Within MES, the situation is not that simple for IH mode.^{65,66} A slight change in VEV arrangement is required in IH mode in order to give correct observed phenomenology.⁶⁵ A new triplet flavon φ'' with VEV alignment along $\langle \varphi'' \rangle \sim (2v, -v, -v)$ is introduced, which modifies the Dirac neutrino mass matrix. Particles and charges under symmetry groups ($SU(2) \times A_4 \times Z_4 \times Z_2$) are shown in table 3. The modified Yukawa Lagrangian for the M_D is given by,

$$\mathcal{L}_{\mathcal{M}_D} = \frac{y_2}{\Lambda} (\bar{l} \tilde{H}_1 \zeta)_1 \nu_{R1} + \frac{y_2}{\Lambda} (\bar{l} \tilde{H}_1 \varphi'')_{1''} \nu_{R2} + \frac{y_3}{\Lambda} (\bar{l} \tilde{H}_1 \varphi)_1 \nu_{R3}. \quad (6)$$

^eWe have assumed the VEV of the Higgs doublets to be identical for simplicity.

Table 3. Particle content and their charge assignments under SU(2), A_4 and $Z_4 \times Z_3$ groups for IH.

Particles	l	e_R	μ_R	τ_R	H_1	H_2	ζ	φ	φ''	ξ	ξ'	ν_{R1}	ν_{R2}	ν_{R3}	S	χ
SU(2)	2	1	1	1	2	2	1	1	1	1	1	1	1	1	1	1
A_4	3	1	$1''$	$1'$	1	1	3	3	1	$1'$	1	1	$1'$	1	$1''$	$1'$
Z_4	1	1	1	1	1	i	1	1	i	1	-1	1	-i	-1	i	-i
Z_3	1	1	1	1	ω	1	1	1	1	ω^2	ω^2	ω^2	ω	ω^2	ω^2	ω

Except the Dirac Lagrangian, other Lagrangian will retain the same form as per the equation 1. The Dirac neutrino mass matrix takes new structure as,

$$M'_D = \begin{pmatrix} D_1 & -D_1 & D_2 \\ 0 & -D_1 & D_2 \\ 0 & 2D_1 & D_2 \end{pmatrix}. \quad (7)$$

Similar to the NH case, this Dirac neutrino mass matrix also get modified by adding the M_P matrix. We have shown the complete matrix structure for both the mass ordering in the table 4

3. Numerical Analysis

Following the minimal extended seesaw (MES) framework we set up active and sterile neutrino mass matrices. In MES scenario three extra right-handed neutrinos and one additional gauge singlet chiral field S is introduced along with the SM particles. The MES Lagrangian for neutrino mass terms is given by,

$$-\mathcal{L}_{\mathcal{M}} = \bar{\nu}_L M_D \nu_R + \frac{1}{2} \bar{\nu}_R^c M_R \nu_R + \bar{S}^c M_S \nu_R + h.c., \quad (8)$$

Here, M_D and M_R are 3×3 Dirac and Majorana neutrino mass matrices respectively with M_S being a 1×3 matrix. A detailed discussion on MES has already been carried out in previous works.^{18, 65, 66} The active neutrino mass matrix within MES framework is given by,

$$m_\nu \simeq M_D M_R^{-1} M_S^T (M_S M_R^{-1} M_S^T)^{-1} M_S (M_R^{-1})^T M_D^T - M_D M_R^{-1} M_D^T, \quad (9)$$

and the keV scaled sterile neutrino mass as,

$$m_s \simeq -M_S M_R^{-1} M_S^T. \quad (10)$$

With these (9) and (10) equations, we established the active and sterile mass structures for both the NH as well as IH.

We diagonalize the active neutrino mass matrix using the popular U_{PMNS} matrix.⁸⁵ The diagonalize neutrino mass matrix M_ν is achieved as,

$$\text{Diag}(m_1, m_2, m_3) = U_{PMNS} M_\nu U_{PMNS}^T, \quad (11)$$

where m_i (for $i = 1, 2, 3$) stands for three active neutrino masses. The leptonic mixing matrix is parameterized as,

$$U_{PMNS} = \begin{pmatrix} c_{12}c_{13} & s_{12}c_{13} & s_{13}e^{-i\delta} \\ -s_{12}c_{23} - c_{12}s_{23}s_{13}e^{i\delta} & c_{12}c_{23} - s_{12}s_{23}s_{13}e^{i\delta} & s_{23}c_{13} \\ s_{12}s_{23} - c_{12}c_{23}s_{13}e^{i\delta} & -c_{12}s_{23} - s_{12}c_{23}s_{13}e^{i\delta} & c_{23}c_{13} \end{pmatrix}.P. \quad (12)$$

We use abbreviations as $c_{ij} = \cos \theta_{ij}$, $s_{ij} = \sin \theta_{ij}$ where θ_{ij} stands for leptonic mixing angles with $i, j = 1, 2, 3 (i \neq j)$. P would be a unit matrix $\mathbf{1}$ in the Dirac case but in the Majorana case $P = \text{diag}(1, e^{i\alpha}, e^{i(\beta+\delta)})$. δ and (α, β) are the Dirac and Majorana CP phases respectively.

The inclusion of one extra generation of neutrino along with the active neutrinos lead us to the final 4×4 neutrino mixing matrix for the active-sterile mixing as,

$$V \simeq \begin{pmatrix} (1 - \frac{1}{2}WW^\dagger)U_{PMNS} & W \\ -W^\dagger U_{PMNS} & 1 - \frac{1}{2}W^\dagger W \end{pmatrix}, \quad (13)$$

where $W = M_D M_R^{-1} M_S^T (M_S M_R^{-1} M_S^T)^{-1}$ is a 3×1 matrix guided by the strength of the active-sterile mixing *i.e.*, the ratio of $\frac{\mathcal{O}(M_D)}{\mathcal{O}(M_S)}$. In the view of new physics contribution, the trivial 3×3 unitary leptonic mixing matrix, U_{PMNS} may slightly deviate from its generic unitarity behaviour.^{86,87} Generally the active and sterile mixing lead to non-unitarity in the U_{PMNS} matrix. However, a minimal mixing between the active-sterile neutrinos is considered in our study, which doesn't bother the active neutrino scenario. Moreover, the U_{PMNS} is constrained to be unitary at the $\mathcal{O}(10^{-2})$ level by the current electroweak precision measurements and neutrino oscillation data.⁸⁸ The sterile neutrino with mass of the order keV , can be added to the standard 3-neutrino mass states in NH: $m_1 \ll m_2 < m_3 \ll m_4$ as well as IH: $m_3 \ll m_1 < m_2 \ll m_4$. The diagonalized structure for neutrino mass matrix are modified as $m_\nu^{NH} = \text{diag}(0, \sqrt{\Delta m_{21}^2}, \sqrt{\Delta m_{21}^2 + \Delta m_{32}^2}, \sqrt{\Delta m_{41}^2})$ and $m_\nu^{IH} = \text{diag}(\sqrt{\Delta m_{31}^2}, \sqrt{\Delta m_{21}^2 + \Delta m_{31}^2}, 0, \sqrt{\Delta m_{43}^2})$ respectively for NH and IH mass pattern. Within the generic MES framework, the lightest neutrino mass is zero in both the mass ordering.¹⁸ Here, $\Delta m_{41}^2 (\Delta m_{43}^2)$ is the active-sterile mass square difference for NH and IH respectively.

We have assigned fixed non-degenerate values for the right-handed neutrino mass parameters as $R_1 = \times 10^{12}$ GeV, $R_2 = 10^{13}$ GeV and $R_3 = 5 \times 10^{13}$ GeV so that they can demonstrate favourable thermal leptogenesis without effecting the neutrino parameters. The mass matrix generated from eq. (11) gives rise to complex parameters due to the presence of Dirac and the Majorana phases. As the leptonic CP phases are still unknown, we vary them within their allowed 3σ ranges $(0, 2\pi)$. We solved the model parameters of the active mass matrix using current global fit 3σ values for the light neutrino parameters, taken from.⁷⁶

In this work we mainly focus on validating MES to study observable like neutrino-less double beta decay, dark matter and baryogenesis in presence of a keV sterile neutrino (m_S) and finally we will try to find correlation among those observable, which we have discussed in following sub-sections.

Table 4. The active and sterile neutrino mass matrices and corresponding Dirac (M_D), Majorana (M_R) and sterile (M_S) mass matrices for NH and IH mode. The active-sterile mixing matrices (W) and sterile mass for NH and IH mass pattern are also shown in respective columns.

Structures	$-m_\nu$	m_s (keV)	W
Normal Hierarchy			
$M_R = \begin{pmatrix} R_1 & 0 & 0 \\ 0 & R_2 & 0 \\ 0 & 0 & R_3 \end{pmatrix}$	$\begin{pmatrix} \frac{D_1^2}{R_2} + \frac{(D_2+P)^2}{R_3} & \frac{D_1(D_1+P)}{R_2} + \frac{D_2(D_2+P)}{R_3} & \frac{D_1^2}{R_2} + \frac{D_2(D_2+P)}{R_3} \\ \frac{D_1(D_1+P)}{R_2} + \frac{D_2(D_2+P)}{R_3} & \frac{(D_1+P)^2}{R_2} + \frac{D_2^2}{R_3} & \frac{D_1(D_1+P)}{R_2} + \frac{D_2^2}{R_3} \\ \frac{D_1^2}{R_2} + \frac{D_2(D_2+P)}{R_3} & \frac{D_1(D_1+P)}{R_2} + \frac{D_2^2}{R_3} & \frac{D_1^2}{R_2} + \frac{D_2^2}{R_3} \end{pmatrix}$	$\simeq \frac{G^2}{\lambda_1 v}$	$\begin{pmatrix} \frac{D_1}{G} \\ 0 \\ \frac{P}{G} \end{pmatrix}$
$M_D = \begin{pmatrix} D_1 & D_1 & D_2+P \\ 0 & D_1+P & D_2 \\ P & D_1 & D_2 \end{pmatrix}$			
$M_S = (G \ 0 \ 0)$			
Inverted Hierarchy			
$M_R = \begin{pmatrix} R_1 & 0 & 0 \\ 0 & R_2 & 0 \\ 0 & 0 & R_3 \end{pmatrix}$	$\begin{pmatrix} \frac{D_1^2}{R_2} + \frac{(D_2+P)^2}{R_3} & \frac{D_1(D_1-P)}{R_2} + \frac{D_2(D_2+P)}{R_3} & \frac{-2D_1^2}{R_2} + \frac{D_2(D_2+P)}{R_3} \\ \frac{D_1(D_1-P)}{R_2} + \frac{D_2(D_2+P)}{R_3} & \frac{(D_1-P)^2}{R_2} + \frac{D_2^2}{R_3} & \frac{-2D_1(D_1-P)}{R_2} + \frac{D_2^2}{R_3} \\ \frac{-2D_1^2}{R_2} + \frac{D_2(D_2+P)}{R_3} & \frac{-2D_1(D_1-P)}{R_2} + \frac{D_2^2}{R_3} & \frac{4D_1^2}{R_2} + \frac{D_2^2}{R_3} \end{pmatrix}$	$\simeq \frac{G^2}{\lambda_1 v}$	$\begin{pmatrix} \frac{D_1}{G} \\ 0 \\ \frac{P}{G} \end{pmatrix}$
$M_D = \begin{pmatrix} D_1 & -D_1 & D_2+P \\ 0 & -D_1+P & D_2 \\ P & 2D_1 & D_2 \end{pmatrix}$			
$M_S = (G \ 0 \ 0)$			

3.1. Neutrino-less Double Beta Decay ($0\nu\beta\beta$):

We assumed that, heavy Majorana neutrinos mediate the observed $0\nu\beta\beta$ process at tree-level. Under the SM framework, the decay amplitude is proportional to:^{36,89}

$$\Sigma G_f^2 U_{ei}^2 \gamma_\mu P_R \frac{\not{p} + m_i}{p^2 - m_i^2} \gamma_\nu P_L \simeq \Sigma G_f^2 U_{ei}^2 \frac{m_i}{p^2} \gamma_\mu P_R \gamma_\nu, \quad (14)$$

where, G_F is the Fermi constant, m_i the physical neutrino mass and p is the neutrino virtual momentum such that $p^2 = -(125\text{MeV})^2$. The effective electron neutrino Majorana mass for the active neutrinos in the $0\nu\beta\beta$ process read as,

$$m_{eff}^{3\nu} = m_1|U_{e1}|^2 + m_2|U_{e2}|^2 + m_3|U_{e3}|^2, \quad (15)$$

The phase "effective *electron* neutrino" is used as only electrons were involved in the double decay process. If the SM is extended by n_S extra sterile fermions, the presence of those extra states will modify the decay amplitude which corrects the effective mass as,¹⁷

$$m_{eff} = \sum_{i=1}^{3+n_S} U_{ei}^2 p^2 \frac{m_i}{p^2 - m_i^2}, \quad (16)$$

where, U_{ei} is the $(3+n_S \times 3+n_S)$ matrix with extra active-sterile mixing elements. As we have considered only one sterile state, hence the effective electron neutrinos mass is modified as,¹⁸

$$m_{eff}^{3+1} = m_{eff}^{3\nu} + m_4|\theta_S|^2, \quad (17)$$

where, $|\theta_S|$ is obtained from the first element of the R matrix and m_4 is constrained within $[1-18.5] \text{ keV}^{36}$ satisfying both $0\nu\beta\beta$ and DM phenomenology under MES framework simultaneously.

Many experimental and theoretical progress were made so far and still counting in order to validate the decay process. Interestingly, till date no solid evidences from experiments confirmed $0\nu\beta\beta$ process. However, next-generation experiments⁹⁰⁻⁹⁴ are currently running in pursue of more accurate limit on the effective mass which might solve the absolute mass problem. Recent results from various experiments give strong bounds on the effective mass m_{eff} . Kam-LAND ZEN Collaboration⁹⁵ and GERDA³⁴ which uses Xenon-136 and Germanium-76 nuclei respectively gives the most constrained upper bound upto 90% CL with

$$m_{eff} < 0.06 - 0.165 \text{ eV.}$$

Various ongoing and future experiments with their bounds on effective mass are shown in table 5. Throughout this work, we consider the future sensitivity of m_{eff} up to 0.01 eV.

Table 5. Sensitivity of few past and future experiments with half-life in years.

Experiments (Isotope)	$ m_{eff} $ eV	Half-life (in years)	Ref.
KamLAND-Zen(800 Kg)(Xe-136)	0.025 – 0.08	1.9×10^{25} (90%CL)	95
KamLAND2-Zen(1000Kg)(Xe-136)	< 0.02	1.07×10^{26} (90%CL)	95
GERDA Phase II (Ge-76)	0.09 – 0.29	4.0×10^{25} (90%CL)	34
CUORE (Te-130)	0.051 – 0.133	1.5×10^{25} (90%CL)	91
SNO+ (Te-130)	0.07 – 0.14	$\sim 10^{26-27}$	92
SuperNEMO (Se-84)	0.05 – 0.15	5.85×10^{24} (90%CL)	94
AMoRE-II (Mo-100)	0.017 – 0.03	3×10^{26} (90%CL)	96
EXO-200(4 Year)(Xe-136)	0.075 – 0.2	1.8×10^{25} (90%CL)	97
nEXO(5Yr+5Yr w/Ba Tagging)(Xe-136)	0.005 – 0.011	$\sim 10^{28}$	98

3.2. Dark Matter

Since sterile neutrinos cannot thermalize easily, the most straightforward production mechanism is via mixing with the active neutrinos in the primordial plasma.¹⁴ Depending upon the production mechanism, one can discard the fact that the mixing of active neutrinos cannot generate sterile neutrinos to behave as a dark matter.⁹⁹ Too large mixing between active-sterile correspond to a too large DM density however, we can still consider the possibility by considering very small mixing angles.^{71,100} The DM sterile neutrino production via mixing becomes most efficient at temperatures $T \sim 150 - 500 \text{ MeV}$ ^{14,71,100,101} resulting in the population of warm DM particles. Resonant production^f results into an efficient conversion of an excess of $\nu_e(\bar{\nu}_e)$ into DM neutrinos S .^{102,103} One important thing to keep in mind

^fResonantly produced (RP) sterile neutrinos are typically much colder and the dispersion of their momentum distribution is also much smaller than thermal. Therefore, in some sense resonantly

here is that, the overproduction of dark matter must be avoided to make them experimentally achievable. With proper adjustment of the *critical temperature* (T_c)^g, we could possibly avoid the overproduction of dark matter abundance. Above the critical temperature, the mixing parameter, $\sin^2 2\theta_S$ from eq. (20) got heavily suppressed, if sterile mass either vanishes or very high at that temperature.^{71,104} If one considers the mixing angle to be a dynamical quantity, then it's not possible to obtain a relic of that quantity. Notwithstanding, in this work, we have considered a tiny static active-sterile mixing angle ($\theta_S < 10^{-6}$) such that they remain in the Universe as DM relic.^{100,105,106} The important thing to note here is that, sterile neutrino DM is practically always produced out of thermal equilibrium. Therefore, its primordial momentum distribution is in general, not given by a Fermi-Dirac distribution. Indeed, sterile neutrinos in equilibrium have the same number density as ordinary neutrinos, *i.e.*, 112 cm^3 . With the sterile neutrino mass above 0.4 keV would lead to the energy density today $\rho_{sterile,eq} \simeq 45 \text{ keV/cm}^3$, which significantly exceeds the critical density of the Universe $\rho_{crit} = 10.5 h^2 \text{ keV/cm}^3$. Therefore, sterile neutrino DM cannot be a thermal relic (unless entropy dilution is exploited), and its primordial properties are in general different from such a particle. Detailed discussion on dark matter production mechanism is beyond the scope of this paper, for more comprehensive study one may refer to.^{71,100,104}

The most important criterion for a DM candidate is its stability, at least on the cosmological scale. The lightest sterile neutrino is not stable and may decay into SM particles. In the presence of sterile neutrinos, the leptonic weak neutral current is not diagonal in mass eigenstates,¹⁰⁷ so the S can decay at tree-level via Z -exchange, as $S \rightarrow \nu_i \bar{\nu}_j \nu_j$, where ν_i, ν_j are mass eigenstates. The keV sterile neutrino decaying to the SM neutrinos (flavor eigenstates) via $S \rightarrow \nu_\alpha \nu_\beta \bar{\nu}_\beta$ gives the decay width as,^{107,108}

$$\Gamma_{S \rightarrow 3\nu} = \frac{G_F^2 m_S^5}{96\pi^3} \sin^2 \theta_S = \frac{1}{4.7 \times 10^{10} \text{ sec}} \left(\frac{m_S}{50 \text{ keV}} \right)^5 \sin^2 \theta_S, \quad (18)$$

where, θ_S and m_S represents the active-sterile mixing angle and sterile mass respectively. This decay width must give a lifetime of the particle much longer than the age of the Universe. This put a bound on the mixing angle such that,

$$\theta_S < 1.1 \times 10^{-7} \left(\frac{50 \text{ keV}}{m_S} \right)^5. \quad (19)$$

The mass squared difference emerging out of this bound is already much smaller than the current solar mass squared difference. To overcome this short come, either we use another sterile neutrino into the picture or consider one loop-mediated radiative decay process of $S \rightarrow \nu + \gamma$. This would put a stronger bound than the earlier $S \rightarrow 3\nu$ decay process leading to a monochromatic X-ray line signal. However, as discussed in literature,¹⁰⁰ the decay rate is negligible on the cosmological

produced sterile neutrinos behave as a mixture of a cold and warm DM (CWDM) over some range of scales¹⁰⁰

^gTemperature at which dark matter production starts.

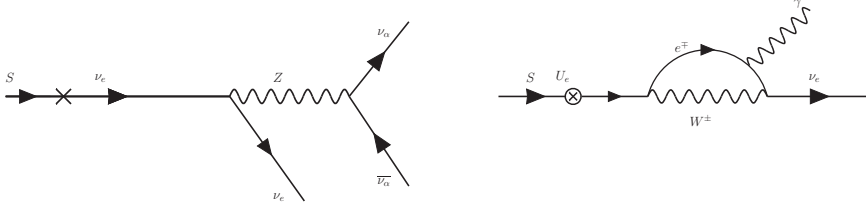


Fig. 1. $S \rightarrow \nu_\alpha \nu_\beta \bar{\nu}_\beta$ (left) and $S \rightarrow \nu + \gamma$ (right) decay processes of the sterile neutrino.¹⁰⁰ Left figure gives dominant decay channel to three active neutrinos/anti-neutrinos and right figure shows loop mediated radiative decay channel that allows to look for the signal of sterile neutrino DM in the spectra of DM dominated objects.

scale because of the small mixing angle. The decay rate for the $S \rightarrow \nu + \gamma$ process is given as^{109, 110}

$$\Gamma_{S \rightarrow \nu \gamma} \simeq 1.32 \times 10^{-32} \left(\frac{\sin^2 2\theta_S}{10^{-10}} \right) \left(\frac{m_S}{keV} \right)^5 \quad (20)$$

Relic abundance of the Universe can be worked out starting from the Boltzmann equation. We used results from^{100, 109, 110} to check whether our model can verify the observed relic abundance of DM if we consider the sterile neutrino mass in keV range. The working formula for relic abundance is given by,

$$\Omega_{DM} h^2 \simeq 0.3 \left(\frac{\sin^2 2\theta_{S\nu}}{10^{-10}} \right) \left(\frac{m_S}{100keV} \right)^2, \quad (21)$$

with $\theta_{S\nu}$ is the sum of all the active-sterile mixing angles and m_S represents the keV ranged sterile neutrino mass. As seen from the above equations, decay rate and the relic abundance depend on the mixing and mass of the DM candidate. Hence, the same set of model parameters that are supposed to produce correct neutrino phenomenology can also be used to evaluate relic abundance and decay rate of the sterile neutrino.

3.3. *Baryogenesis via Leptogenesis:*

In the early Universe, there is a rapid violation of $B + L$, at temperatures above the electroweak phase transition (EWPT),¹¹¹ which converts the lepton asymmetry to baryon asymmetry. Both the baryon number (B) and lepton number (L) are independently conserved in the renormalizable SM Lagrangian. However, there are non-perturbative gauge field configurations¹¹² due to chiral anomaly, which ignites the anomalous $B + L$ violation^h. This conversion of lepton asymmetry to baryon asymmetry via $B + L$ violation is popularly termed as "sphalerons"¹¹³ process. In this work, we consider the decay of lightest RH neutrino ν_{R1} ($L = 1$) to a SM lepton l ($L = 1$) and Higgs H ($L = 0$) and this decay process of $\nu_{R1} \rightarrow lH$, will violate

^h $B - L$ is already conserved.

lepton number by two units ($\Delta L = 2$). Following the parametrization from,⁵⁷ the working formula of baryon asymmetry produced is given by,

$$Y_B = ck \frac{\epsilon_{11}}{g_*}, \quad (22)$$

where, c is the conversion factor. It measures the fraction of lepton asymmetry being converted to baryon asymmetry which is approximately 12/37. The term k is the dilution factor due to wash out processes, and this is parametrized as,

$$\begin{aligned} k &\simeq \sqrt{0.1K} \exp\left[\frac{-4}{3(0.1K)^{0.25}}\right], \quad \text{for } K \geq 10^6, \\ &\simeq \frac{0.3}{K(\ln K)^{0.6}}, \quad \text{for } 10 \leq K \leq 10^6, \\ &\simeq \frac{1}{2\sqrt{K^2 + 9}}, \quad \text{for } 0 \leq K \leq 10. \end{aligned} \quad (23)$$

Here, K is defined as,

$$K = \frac{\Gamma_1}{H(T = M_{\nu_{R1}})} = \frac{(h^\dagger h)_{11} M_{\nu_{R1}}}{8\pi} \frac{M_{Plank}}{1.66\sqrt{g_*} M_{\nu_{R1}}^2}, \quad (24)$$

where, Γ_1 is the decay width of ν_{R1} , defined as, $\Gamma_1 = \frac{(h^\dagger h)_{11} M_{\nu_{R1}}}{8\pi}$ and the Hubble constant at $T = M_{\nu_{R1}}$ is defined as $H(T = M_{\nu_{R1}}) = \frac{M_{Plank}}{1.66\sqrt{g_*} M_{\nu_{R1}}^2}$. The quantity g_* is the mass-less relativistic degree of freedom in the thermal bath and it's value is approximately around 110. The most important term is the lepton asymmetry term " ϵ_{11} " that produced by the decay of the lightest RH neutrino ν_{R1} .

Decay of the ν_{R1} must have a lepton number violating process with different decay rate to final state with particle and anti-particle, otherwise the lepton asymmetry would be vanished. Asymmetry produced by the decay of ν_{R1} in lepton flavor α produced is defined as,

$$\epsilon_{\alpha\alpha} = \frac{\Gamma(\nu_{R1} \rightarrow l_\alpha H) - \Gamma(\nu_{R1} \rightarrow \bar{l}_\alpha \bar{H})}{\Gamma(\nu_{R1} \rightarrow l H) + \Gamma(\nu_{R1} \rightarrow \bar{l} \bar{H})}, \quad (25)$$

where $\bar{l}_{(\alpha)}$ is the antiparticle of $l_{(\alpha)}$ and H is the Higgs doublet. With non-degenerate RH massⁱ, we carried out our numerical analysis from the work of¹¹⁴ and obtained the asymmetry term as,

$$\begin{aligned} \epsilon_{\alpha\alpha} &= \frac{1}{8\pi} \frac{1}{[h^\dagger h]_{11}} \sum_j^{2,3} \text{Im}(h_{\alpha 1}^*) (h^\dagger h)_{1j} h_{\alpha j} g(x_j) \\ &+ \frac{1}{8\pi} \frac{1}{[h^\dagger h]_{11}} \sum_j^{2,3} \text{Im}(h_{\alpha 1}^*) (h^\dagger h)_{1j} h_{\alpha j} \frac{1}{1 - x_j}, \end{aligned} \quad (26)$$

ⁱFor degenerate RH mass with mass spiting equal to decay width lead to the case of resonant leptogenesis.

where $x_j \equiv \frac{M_j^2}{M_1^2}$ and within the SM $g(x_j)$ is defined as ,

$$g(x_j) = \sqrt{x_j} \left(\frac{2 - x_j - (1 - x_j^2) \ln(1 + x_j/x_j)}{1 - x_j} \right). \quad (27)$$

When we take sum over α , the second line from equation (26) violates single lepton flavors, however, it conserves the total lepton number and it vanishes.

$$\epsilon_{11} \equiv \sum_{\alpha} \epsilon_{\alpha\alpha} = \frac{1}{8\pi} \frac{1}{[h^\dagger h]_{11}} \sum_j^{2,3} \text{Im}[(h^\dagger h)_{1j}]^2 g(x_j) \quad (28)$$

The h used here is the Yukawa matrix generated from the Dirac neutrino mass matrix and the corresponding index in the suffix conveys the position of respective matrix element.

We constructed the Yukawa matrix from the solved model parameters D_1, D_2 and P , which is related to the 3×3 Dirac neutrino mass matrix. The K value within our study fell in the range $10 \leq K \leq 10^6$; thus, we have to go for the second parametrization of the dilution factor from equation (23). Now, the baryon asymmetry of the Universe can be calculated from equation (22), followed by the evaluation of lepton asymmetry using the equation (28).

4. Results

Under the hypothesis that future experiments will verify the existence of at least one heavy sterile neutrino in keV range, we work out the possibility of its effect on $0\nu\beta\beta$ and verifying the fact that this sterile neutrino could behave as DM within the mass range of (1-18.5) keV . We have plotted effective neutrino mass (m_{eff}) against the lightest neutrino mass ($m_{lightest}$) in fig. 2. The horizontal gray line gives the future sensitivity of upper bound on effective mass up to 10^{-2} eV, and the vertical blue line gives the upper bound on the sum of the active neutrino masses (0.17 eV). In the upper part of fig. 2, NH (black) and IH (orange) contributions are coming only from the active neutrinos, whereas, in lower two figures, NH and IH contributions are shown separately in the presence of m_S . In presence of the sterile neutrino, one can observe a wider and improved data range in both the mass ordering. These extra contributions and improvements in effective mass are due to the sterile neutrino mass (m_S) and the active-sterile mixing (θ_S). In fig. 3, we completed the same analysis of m_{eff} vs. $m_{lightest}$ for different orders of active-sterile mixing element. Very interesting results are observed from both NH and IH mode. For $m_4|\theta_S|^2 > 10^{-4}$ keV , $0\nu\beta\beta$ fails the future experimental bound. From these results, we get the upper bound on the active-sterile mixing angles and it is also obvious from the fact that the active-sterile mixing element must be very small otherwise there would be an overproduction of dark matter in our Universe.⁷¹

Variation of Yukawa couplings with the baryogenesis result are shown in fig. 4. The red dots represent NH and the blue dots represent IH respectively. The green

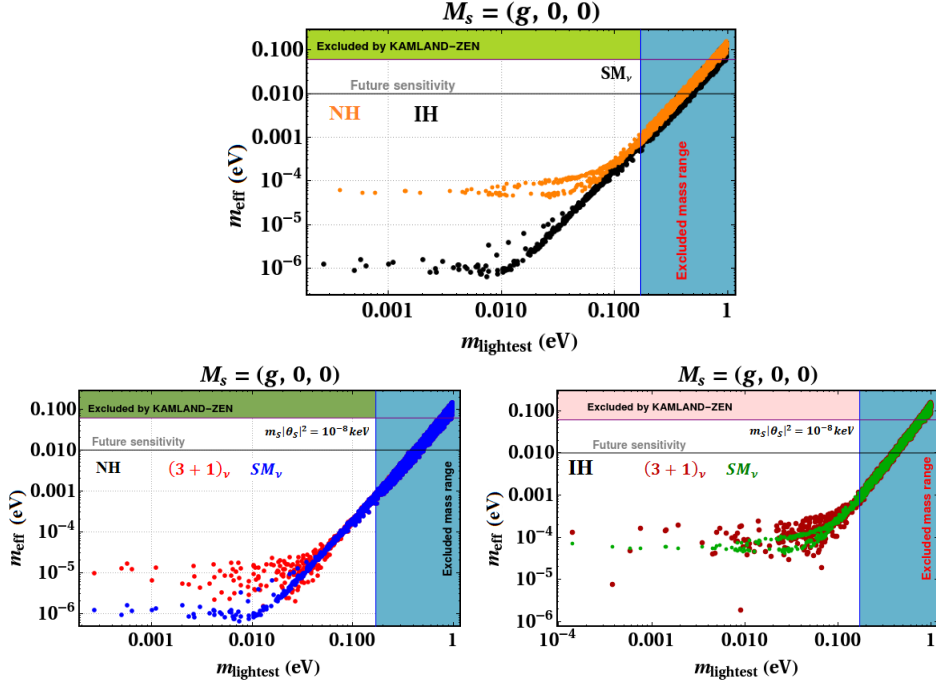


Fig. 2. Variation of effective neutrino mass vs. the lightest neutrino mass. The upper plot represents the contribution from the active neutrinos only. The lower two plots represent NH and IH respectively, for both active and active+sterile contributions. Horizontal gray line and vertical blue line represent the future m_{eff} bound and sum of the active masses respectively. In presence of sterile neutrino, a much wider and significant impact is visible on the bottom plots. In both the mass orderings we have fixed the mixing element $m_S|\theta_S|^2 = 10^{-8} keV$.

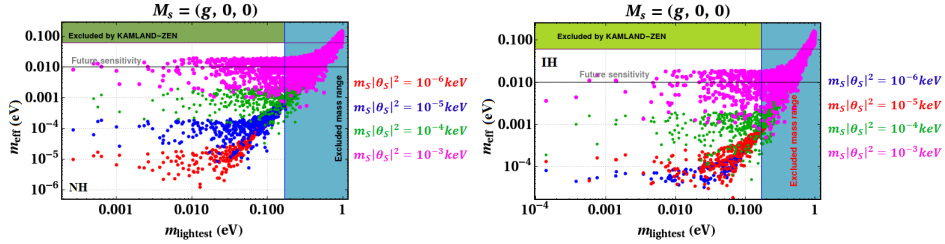


Fig. 3. Variation of effective mass for different ranges of active-sterile mixing angle. The left plot represents the NH mode while the right one represents the IH mode. In both the mass patterns, $m_S|\theta_S|^2 > 10^{-4} keV$ fails to satisfy the future sensitivity bound of effective mass. This result gives upper bound on the active-sterile mixing element " $|\theta_S|^2$ " from the $0\nu\beta\beta$ study.

bar gives the current allowed 3σ value of BAU. As BAU value is highly sensitive to the experimental results, very narrow regions are observed in both the mass ordering satisfy baryogenesis in our model and NH shows more favorable results when we vary BAU with the Yukawa couplings. In current dimension-5 scenario, the

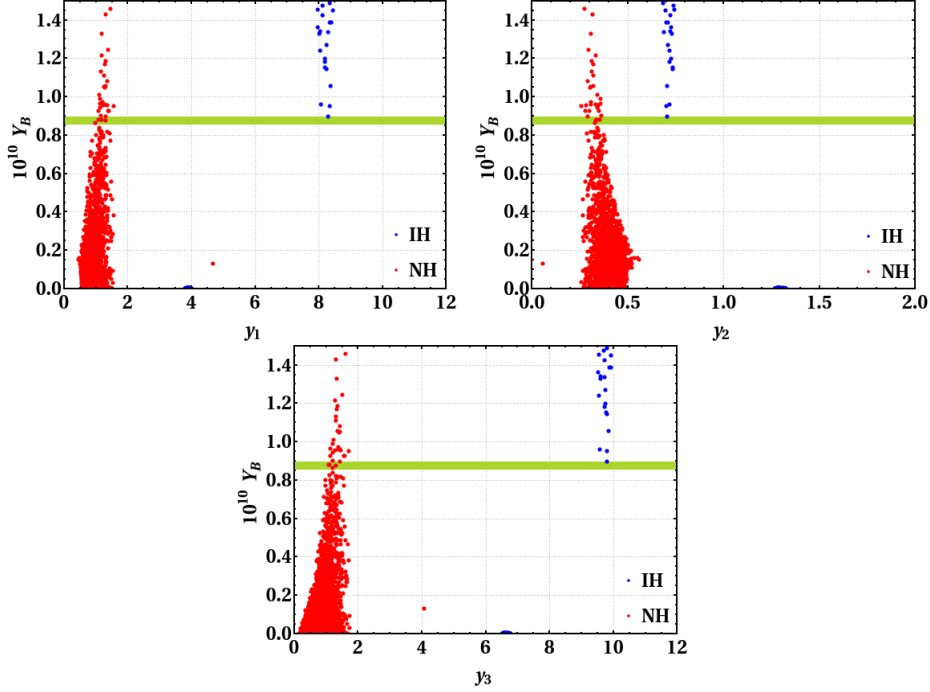


Fig. 4. Variation of Yukawa coupling with BAU in both the mass ordering. Solid green band represents the current BAU value within 3σ range, which is $(8.7 \pm 0.06) \times 10^{-11}$. Red and blue points represents NH and IH mass ordering respectively. Yukawa couplings (y_1, y_2, y_3) satisfying BAU results are achieved around $\mathcal{O}(10^{-1} - 1)$, which are also in accessible range for dimension-5 frameworks. Stringent regions on the Yukawa couplings are due to recent bounds on the light neutrino parameters.

Yukawa coupling of $\mathcal{O}(10^{-2} - 1)^{115-117}$ are in acceptable range. Strong constrained regions in fig. 4 are due to the bounds on light neutrino parameters imposed by the Yukawa matrix involved in the baryogenesis calculation. These constrained regions of Yukawa couplings also put stringent bounds on the light neutrino parameters. For example, within NH, for large $y_3 (\geq 2.0)$, Δm_{31}^2 value exceed the current upper bound of 3σ value, whereas small $y_3 (\leq 0.2)$, Δm_{31}^2 value goes beneath the lower 3σ bound. Parallel to the $0\nu\beta\beta$ study, we have also examined dark matter signature of the keV sterile neutrino in fig. 5. Decay width (Γ) and relic abundance of the sterile neutrino ($\Omega_{DM} h^2$) are plotted against the sterile mass (m_S) for both the mass ordering. Sterile neutrinos to behave as a DM, their lifetime must be greater than the age of the Universe so that their remnants remain in the Universe; hence, the decay width of the particle must be very less. In our study, we have considered the upper limit of decay width to be less than 10^{-28} (sec^{-1}). The sterile neutrino mass is considered in a narrow region, i.e., $(1 - 18.5)$ keV to be a relic particle. Relic abundance obtained in both the mass ordering, satisfy the proper bound with different m_S ranges. The allowed mass range for the sterile neutrino is very nar-

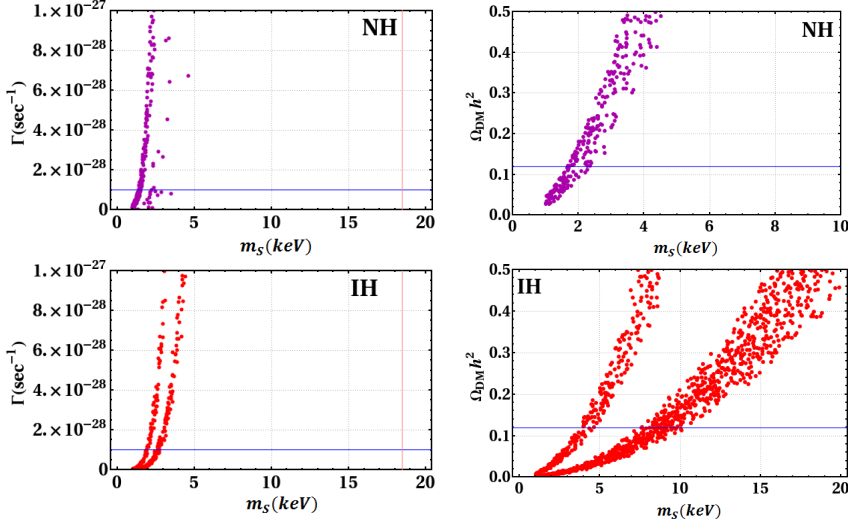


Fig. 5. Variation of decay width (Γ) and the relic abundance ($\Omega_{DM}h^2$) of the Universe vs. the sterile neutrino mass (m_S). Sterile neutrino to behave as a dark matter, $m_S \simeq 7.1 \text{ keV}$ and lifetime $\tau_{DM}(\Gamma^{-1}) \simeq 10^{27.8 \pm 0.3} \text{ sec}$ are suggested from the recent discovery of $E = 3.55 \text{ keV}$ line in the X-ray spectra of galaxy cluster.^{72,74} For decay width plots, the blue lines give the upper limit of the decay width which is considered to be $\Gamma < 10^{-28} \text{ sec}$. On the other hand for relic abundance plots, the solid blue line gives the current best fit value for relic abundance of a particle to behave as a dark matter ($\Omega_{DM}h^2 = 0.119$). m_S around 1-3 keV is consistent with NH mode and for IH mode the mass ranges are different while satisfying both the decay width and relic abundance. In IH mode, m_S around 1-3 keV is consistent with the upper bound of decay width, while m_S between 4-10 keV satisfy the current relic abundance value.

row (1 – 3) keV in case of NH mode, while a broad mass spectrum satisfies the upper relic abundance bound in IH mode (1 – 10) keV. Recent results suggested $m_S \simeq 7.1 \text{ keV}$ and lifetime $\tau_{DM} \simeq 10^{27.8 \pm 0.3} \text{ sec}$.⁷⁴ Even though the decay width and the relic abundance of the sterile neutrino are satisfied in both the mass ordering, NH results are more consistent with sterile mass within (1-3) keV. On the other hand in case of IH mode, relic abundance limit is within the sterile mass range from 4 keV to 10 keV, while decay width is satisfied with a small mass up to 3 keV.

We also study the results for baryogenesis via the mechanism of thermal leptogenesis and showed a co-relation among other observable. In fig. 6, we varied the Dirac delta phase (δ) with the baryon asymmetry of the Universe calculated in our model in both the mass orderings. Both these results show the validity of BAU within our model. Similar results can be seen from fig. 7, where we project BAU in between Dirac and Majorana phases for NH mode only. Co-relation among the effective neutrino mass in the presence of keV sterile neutrino with the BAU is also shown in fig. 8. Since the Dirac CP phase has influence in $0\nu\beta\beta$ as well as in BAU, we added contour plot with m_{eff} and δ along the axes and projected BAU value in the Z-plane in fig. 9. Constrained regions in the Dirac CP phase are observed in both the mass orderings. As we can see from the legends on right-hand side of

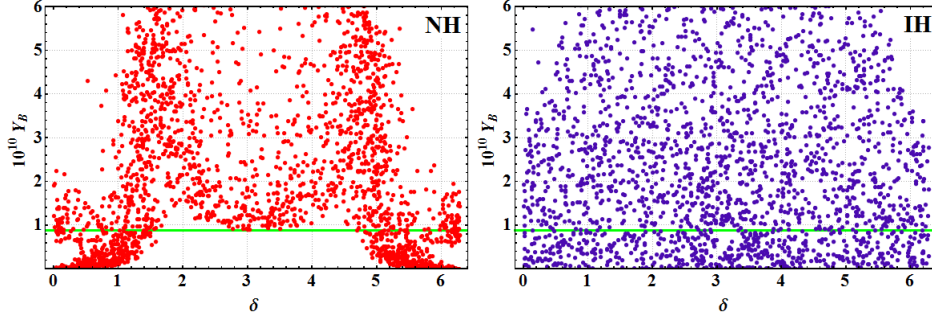


Fig. 6. Variation of the Dirac delta phase with Y_B in both the mass ordering. The solid green band represents the current BAU value, $Y_B = (8.7 \pm 0.06) \times 10^{-11}$. Both the mass orderings satisfy baryogenesis in our model and correlate with δ

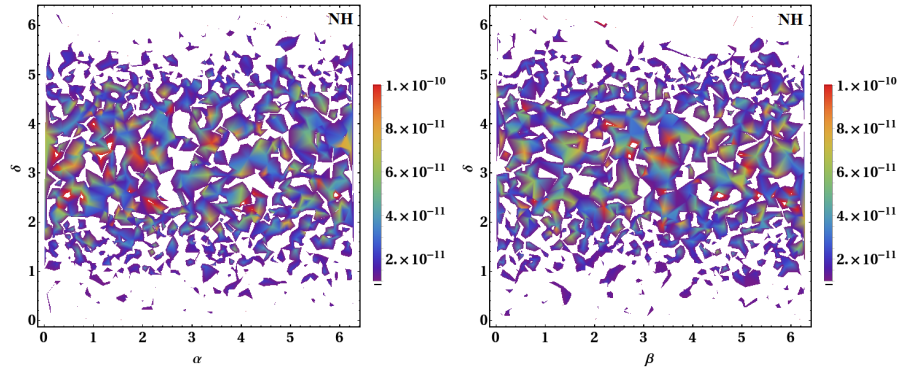


Fig. 7. Projection of BAU value (Y_B) between Dirac CP-phase (δ) along X-axis and Majorana phases (α and β respectively) along Y-axis. Current BAU value range is around the red-orange colour band and this constrains the Dirac CP phase (δ) in between the numerical values (2.0-4.0).

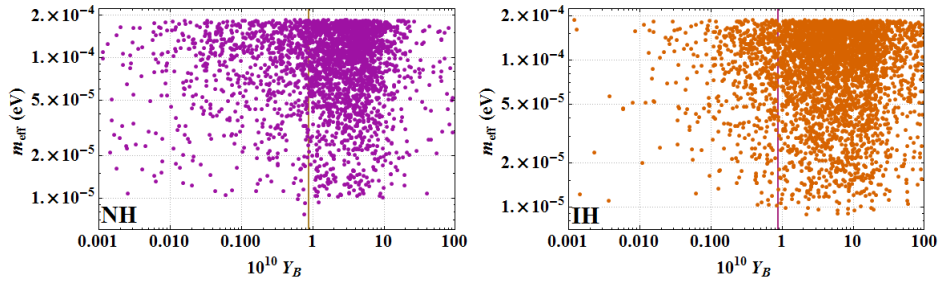


Fig. 8. Correlation between effective neutrino mass (m_{eff}) with Y_B in NH and IH respectively. Solid vertical band represents the current BAU value, which is $(8.7 \pm 0.06) \times 10^{-11}$. In both the cases, m_{eff} lie well below the current upper bound and the solid vertical line indicates successful execution of baryogenesis and $0\nu\beta\beta$ in the model.

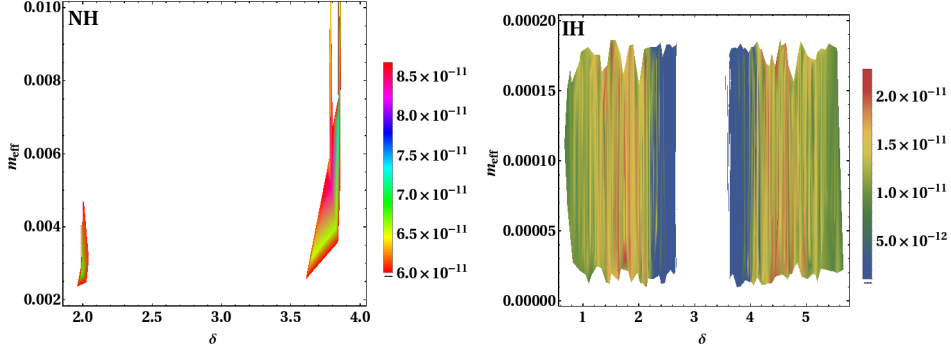


Fig. 9. Projection of BAU value (Y_B) in a frame representing effective mass (m_{eff}) along Y-axis and the Dirac CP-phase (δ) along X-axis. A precise constrained range for the Dirac CP-phase value around 3.5-4.0 is obtained for NH mode. Whereas IH mode failed to reflect the exact Y_B value.

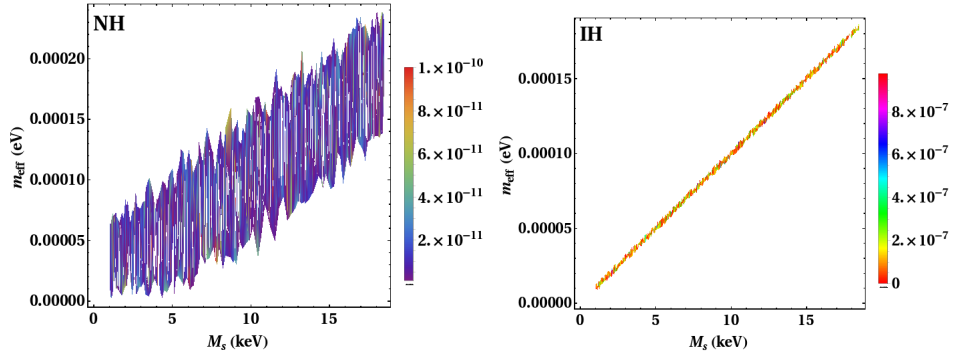


Fig. 10. Projection of Y_B in a frame representing effective mass (m_{eff}) along Y-axis and sterile mass (m_S in keV) along X-axis. Here also Y_B is much higher than its current bound in the IH mode and fails to correlate with m_{eff} and m_S . On the other hand NH was able to project the BAU bound successfully, however, very small regions are observed.

the figure, that IH pattern failed to project the current observed value of BAU in a frame of m_{eff} Dirac-CP phase δ . We also present another contour plots in fig. 10, where a measured BAU is projected in the frame between sterile neutrino mass (m_S) and effective electron neutrino mass. Since BAU results are very sensitive to the experiments, very narrow regions are observed. We can see that IH mode is almost ruled out in presence of sterile mass and mixing while we get some region satisfying current BAU bound in NH mode.

5. Conclusion

In this work, we study the viability of keV sterile neutrino to behave as a warm dark matter and giving an observable effect in $0\nu\beta\beta$ and baryogenesis via the mechanism of thermal leptogenesis. We use A_4 based flavor model with discrete $Z_4 \times Z_3$ to

construct desired Yukawa coupling matrices. Here, the Dirac neutrino mass M_D is a 3×3 complex matrix, the Majorana mass matrix M_R , which arises due to the coupling of right-handed neutrinos is also a 3×3 complex symmetric diagonal matrix with non-degenerate values. A singlet gauge fermion S is considered which couples with the right-handed neutrino, hence produces a single row 1×3 M_S matrix with one non-zero entry. The Dirac neutrino mass matrix, M_D , is modified using a matrix, M_P , which is generated via the same fashion as M_D to make the active mass matrix $\mu - \tau$ asymmetric. Few interesting points based on the results are discussed as follows,

- Presence of an extra heavy sterile flavor has a significant impact on effective neutrino mass. One can find a broader effective mass range in the active-sterile case than the active neutrino case. Normal hierarchy (NH) is more favourable than the inverted hierarchy (IH) mode for $0\nu\beta\beta$ in this MES framework.
- Consequential bound on active-sterile mixing angle is obtained for future sensitivity in effective mass from fig. 3, which restricts the upper bound on the mixing element up to 10^{-4} for $|\theta_S|^2$.
- In fig. 4, strongly constrained regions for the Yukawa couplings are obtained through baryogenesis calculation, which by the by gives strict bounds on the choice model parameters.
- Dark matter analysis results from decay width and relic abundance restricts sterile neutrino mass within few keV to behave as dark matter. Among different bounds for thermal relic mass for the sterile neutrino, very few results are consistent with X-ray observations. Lyman- α forest of high resolution quasar spectra with hydrodynamical N-body simulations gives bounds ranging from $m_S \geq 1.8 keV$ to $m_S \geq 3.3 keV$.¹¹⁸⁻¹²⁰ Regardless, these bounds may vary depending upon various uncertainties effecting the constraints.¹²¹ Within MES framework, NH predicts sterile mass range from $(1 - 3 keV)$ and IH results for relic abundance gives mass up to $10 keV$ while the decay width constraints the mass within $3 keV$. Hence, from these results we come to a conclusion that with current bounds on hand, sterile neutrino as a dark matter in minimal extended seesaw is still an unsettled aspect. A deeper discussion with new bounds on keV sterile neutrino may resolve these issues, which is left for future studies.
- BAU is satisfied in this framework, and NH shows more efficient in producing the observed matter-antimatter density than IH pattern. This model also successfully correlate $0\nu\beta\beta$ with BAU result, which can be found in fig. 8. Projection of BAU on a plane in between effective mass and Dirac CP phase, δ gives significant remark in our study. In fig. 9, one can find that BAU results are constraining δ in both the mass ordering and NH results are more favourable with current BAU value than the IH. Within NH, δ is tightly constrained in between $(2.0 - 4.0)$ value.

- Projection of BAU with sterile mass and effective mass in presence of sterile neutrino in fig. 10 gives an unsatisfactory remark while observing IH. Hence, IH fails to correlate them in a single frame. In spite of the fact that, BAU value is very small, NH manages to project the value along with keV sterile neutrino.
- In NH mode within this model, a constrained bound on the Dirac CP-phase is obtained from baryogenesis study, which can be seen in the density plot of fig. 7 with Majorana phases in the X-axis. Majorana phases cover the whole $0 - 2\pi$ range, whereas the Dirac CP-phase is constrained between the value (2.0 – 4.0) satisfying observed BAU value.

In conclusion, the MES mechanism is analyzed in this work, considering a single flavor of a sterile neutrino in a keV scale. Along with the active and sterile mass generation, this model can also be used to study the connection between effective mass in neutrinoless double beta decay ($0\nu\beta\beta$) in a wider range of sterile neutrino mass, simultaneously addressing the possibility of keV scale sterile neutrino as dark matter particle. Although, results on keV sterile neutrino as a dark matter candidate is still on the verge of uncertainty within the framework of MES. We keep an optimistic hope to get better bounds from future experiments which may establish the same within MES. Results from baryogenesis via the mechanism of thermal leptogenesis are also checked and verified within this model. Finally, we have correlated all these observable under the single framework. Results in NH mass pattern shows better consistency than IH pattern.

Acknowledgements

This work is supported by the Department of Science and Technology, Government of India under project number EMR/2017/001436.

References

1. Super-Kamiokande Collaboration (K. Abe *et al.*), *Phys. Rev.* **D94**, 052010 (2016), [arXiv:1606.07538 \[hep-ex\]](#), doi:10.1103/PhysRevD.94.052010.
2. J. Boger, R. Hahn, J. Rowley, A. Carter, B. Hollebone, D. Kessler, I. Blevis, F. Dalnoki-Veress, A. DeKok, J. Farine *et al.*, *Nuclear Instruments and Methods in Physics Research Section A: Accelerators, Spectrometers, Detectors and Associated Equipment* **449**, 172 (2000).
3. J. Evans, *Advances in High Energy Physics* **2013** (2013).
4. T2K Collaboration (K. Abe *et al.*), *Phys. Rev. Lett.* **107**, 041801 (2011), [arXiv:1106.2822 \[hep-ex\]](#), doi:10.1103/PhysRevLett.107.041801.
5. RENO Collaboration (J. K. Ahn *et al.*), *Phys. Rev. Lett.* **108**, 191802 (2012), [arXiv:1204.0626 \[hep-ex\]](#), doi:10.1103/PhysRevLett.108.191802.
6. Double Chooz Collaboration (Y. Abe *et al.*), *Phys. Rev. Lett.* **108**, 131801 (2012), [arXiv:1112.6353 \[hep-ex\]](#), doi:10.1103/PhysRevLett.108.131801.
7. Daya Bay Collaboration (F. P. An *et al.*), *Phys. Rev. Lett.* **108**, 171803 (2012), [arXiv:1203.1669 \[hep-ex\]](#), doi:10.1103/PhysRevLett.108.171803.

8. LSND Collaboration (C. Athanassopoulos *et al.*), *Phys. Rev. Lett.* **81**, 1774 (1998), [arXiv:nucl-ex/9709006 \[nucl-ex\]](#), doi:10.1103/PhysRevLett.81.1774.
9. LSND Collaboration (C. Athanassopoulos *et al.*), *Phys. Rev. Lett.* **77**, 3082 (1996), [arXiv:nucl-ex/9605003 \[nucl-ex\]](#), doi:10.1103/PhysRevLett.77.3082.
10. LSND Collaboration (A. Aguilar-Arevalo *et al.*), *Phys. Rev.* **D64**, 112007 (2001), [arXiv:hep-ex/0104049 \[hep-ex\]](#), doi:10.1103/PhysRevD.64.112007.
11. J. N. Abdurashitov *et al.*, *Phys. Rev.* **C73**, 045805 (2006), [arXiv:nucl-ex/0512041 \[nucl-ex\]](#), doi:10.1103/PhysRevC.73.045805.
12. C. Giunti and M. Laveder, *Physical Review C* **83**, 065504 (2011).
13. C. Giunti, M. Laveder, Y. Li, Q. Liu and H. Long, *Physical Review D* **86**, 113014 (2012).
14. S. Dodelson and L. M. Widrow, *Phys. Rev. Lett.* **72**, 17 (1994), [arXiv:hep-ph/9303287 \[hep-ph\]](#), doi:10.1103/PhysRevLett.72.17.
15. K. N. Abazajian *et al.* (2012), [arXiv:1204.5379 \[hep-ph\]](#).
16. K. N. Abazajian, *Phys. Rept.* **711-712**, 1 (2017), [arXiv:1705.01837 \[hep-ph\]](#), doi:10.1016/j.physrep.2017.10.003.
17. P. Benes, A. Faessler, F. Simkovic and S. Kovalenko, *Phys. Rev.* **D71**, 077901 (2005), [arXiv:hep-ph/0501295 \[hep-ph\]](#), doi:10.1103/PhysRevD.71.077901.
18. J. Barry, W. Rodejohann and H. Zhang, *JHEP* **07**, 091 (2011), [arXiv:1105.3911 \[hep-ph\]](#), doi:10.1007/JHEP07(2011)091.
19. K. Petraki and A. Kusenko, *Phys. Rev.* **D77**, 065014 (2008), [arXiv:0711.4646 \[hep-ph\]](#), doi:10.1103/PhysRevD.77.065014.
20. A. Abada, V. De Romeri, M. Lucente, A. M. Teixeira and T. Toma, *JHEP* **02**, 169 (2018), [arXiv:1712.03984 \[hep-ph\]](#), doi:10.1007/JHEP02(2018)169.
21. A. Atre, T. Han, S. Pascoli and B. Zhang, *JHEP* **05**, 030 (2009), [arXiv:0901.3589 \[hep-ph\]](#), doi:10.1088/1126-6708/2009/05/030.
22. F. F. Deppisch, P. S. Bhupal Dev and A. Pilaftsis, *New J. Phys.* **17**, 075019 (2015), [arXiv:1502.06541 \[hep-ph\]](#), doi:10.1088/1367-2630/17/7/075019.
23. H. Borgohain, M. K. Das and D. Borah, *JHEP* **06**, 064 (2019), [arXiv:1904.02484 \[hep-ph\]](#), doi:10.1007/JHEP06(2019)064.
24. J. Barry, J. Heeck and W. Rodejohann, *JHEP* **07**, 081 (2014), [arXiv:1404.5955 \[hep-ph\]](#), doi:10.1007/JHEP07(2014)081.
25. W. Rodejohann and H. Zhang, *Phys. Lett.* **B737**, 81 (2014), [arXiv:1407.2739 \[hep-ph\]](#), doi:10.1016/j.physletb.2014.08.035.
26. P. S. Bhupal Dev and A. Pilaftsis, *Phys. Rev.* **D87**, 053007 (2013), [arXiv:1212.3808 \[hep-ph\]](#), doi:10.1103/PhysRevD.87.053007.
27. P. O. Ludl and W. Rodejohann, *JHEP* **06**, 040 (2016), [arXiv:1603.08690 \[hep-ph\]](#), doi:10.1007/JHEP06(2016)040.
28. H. J. de Vega, O. Moreno, E. M. de Guerra, M. R. Medrano and N. G. Sanchez, *Nucl. Phys.* **B866**, 177 (2013), [arXiv:1109.3452 \[hep-ph\]](#), doi:10.1016/j.nuclphysb.2012.08.019.
29. W. H. Furry, *Physical Review* **56**, 1184 (December 1939), doi:10.1103/PhysRev.56.1184.
30. S. Dell’Oro, S. Marocco, M. Viel and F. Vissani, *Adv. High Energy Phys.* **2016**, 2162659 (2016), [arXiv:1601.07512 \[hep-ph\]](#), doi:10.1155/2016/2162659.
31. J. M. Cline, Baryogenesis, in *Les Houches Summer School - Session 86: Particle Physics and Cosmology: The Fabric of Spacetime Les Houches, France, July 31-August 25, 2006*, (2006). [arXiv:hep-ph/0609145 \[hep-ph\]](#).
32. S. M. Bilenky, A. Faessler and F. Simkovic, *Phys. Rev.* **D70**, 033003 (2004),

- arXiv:hep-ph/0402250 [hep-ph], doi:10.1103/PhysRevD.70.033003.
33. S. M. Bilenky and C. Giunti, *Mod. Phys. Lett.* **A27**, 1230015 (2012), arXiv:1203.5250 [hep-ph], doi:10.1142/S0217732312300157.
 34. GERDA Collaboration (M. Agostini *et al.*), *Phys. Rev. Lett.* **120**, 132503 (2018), arXiv:1803.11100 [nucl-ex], doi:10.1103/PhysRevLett.120.132503.
 35. H. Borgohain and M. K. Das, *Phys. Rev.* **D96**, 075021 (2017), arXiv:1709.09542 [hep-ph], doi:10.1103/PhysRevD.96.075021.
 36. A. Abada, . Hernandez-Cabezudo and X. Marcano, *JHEP* **01**, 041 (2019), arXiv:1807.01331 [hep-ph], doi:10.1007/JHEP01(2019)041.
 37. E. Pécontal, T. Buchert, P. Di Stefano, Y. Copin and K. Freese, *European Astronomical Society Publications Series* **36**, 113 (2009).
 38. D. Clowe, M. Bradač, A. H. Gonzalez, M. Markevitch, S. W. Randall, C. Jones and D. Zaritsky, *The Astrophysical Journal Letters* **648**, L109 (2006).
 39. C. Bennett, D. Larson, J. Weiland, N. Jarosik, G. Hinshaw, N. Odegard, K. Smith, R. Hill, B. Gold, M. Halpern *et al.*, *The Astrophysical Journal Supplement Series* **208**, 20 (2013).
 40. Planck Collaboration (P. A. R. Ade *et al.*), *Astron. Astrophys.* **571**, A16 (2014), arXiv:1303.5076 [astro-ph.CO], doi:10.1051/0004-6361/201321591.
 41. J. Yoo, J. Chaname and A. Gould, *Astrophys. J.* **601**, 311 (2004), arXiv:astro-ph/0307437 [astro-ph], doi:10.1086/380562.
 42. P. Pani and A. Loeb, *JCAP* **1406**, 026 (2014), arXiv:1401.3025 [astro-ph.CO], doi:10.1088/1475-7516/2014/06/026.
 43. M. Milgrom, *Astrophys. J.* **270**, 365 (1983), doi:10.1086/161130.
 44. C. Kraus *et al.*, *Eur. Phys. J.* **C40**, 447 (2005), arXiv:hep-ex/0412056 [hep-ex], doi:10.1140/epjc/s2005-02139-7.
 45. V. M. Lobashev *et al.*, *Nucl. Phys. Proc. Suppl.* **91**, 280 (2001), doi:10.1016/S0920-5632(00)00952-X, [,280(2001)].
 46. E. W. Kolb and M. S. Turner, *Front. Phys.* **69**, 1 (1990).
 47. G. Jungman, M. Kamionkowski and K. Griest, *Phys. Rept.* **267**, 195 (1996), arXiv:hep-ph/9506380 [hep-ph], doi:10.1016/0370-1573(95)00058-5.
 48. G. Gelmini and P. Gondolo, *Phys. Rev.* **D74**, 023510 (2006), arXiv:hep-ph/0602230 [hep-ph], doi:10.1103/PhysRevD.74.023510.
 49. G. Servant and T. M. P. Tait, *Nucl. Phys.* **B650**, 391 (2003), arXiv:hep-ph/0206071 [hep-ph], doi:10.1016/S0550-3213(02)01012-X.
 50. J. Bonnevier, H. Melbeus, A. Merle and T. Ohlsson, *Phys. Rev.* **D85**, 043524 (2012), arXiv:1104.1430 [hep-ph], doi:10.1103/PhysRevD.85.109902,10.1103/PhysRevD.85.043524, [Erratum: Phys. Rev.D85,109902(2012)].
 51. L. Lopez Honorez, E. Nezri, J. F. Oliver and M. H. G. Tytgat, *JCAP* **0702**, 028 (2007), arXiv:hep-ph/0612275 [hep-ph], doi:10.1088/1475-7516/2007/02/028.
 52. N. Khan, Exploring Extensions of the Scalar Sector of the Standard Model, PhD thesis, Indian Inst. Tech., Indore (2017).
 53. P. Das, M. K. Das and N. Khan (2019), arXiv:1911.07243 [hep-ph].
 54. Planck Collaboration (N. Aghanim *et al.*) (7 2018), arXiv:1807.06209 [astro-ph.CO].
 55. M. Fukugita and T. Yanagida, *Phys. Lett.* **B174**, 45 (1986), doi:10.1016/0370-2693(86)91126-3.
 56. A. Strumia, Baryogenesis via leptogenesis, in *Particle physics beyond the standard model. Proceedings, Summer School on Theoretical Physics, 84th Session, Les Houches, France, August 1-26, 2005*, (2006), pp. 655–680. arXiv:hep-ph/0608347

- [hep-ph].
57. S. Davidson, E. Nardi and Y. Nir, *Phys. Rept.* **466**, 105 (2008), [arXiv:0802.2962 \[hep-ph\]](#), doi:10.1016/j.physrep.2008.06.002.
 58. P. Di Bari, *Contemp. Phys.* **53**, 315 (2012), [arXiv:1206.3168 \[hep-ph\]](#), doi:10.1080/00107514.2012.701096.
 59. E. Nardi, Y. Nir, E. Roulet and J. Racker, *JHEP* **01**, 164 (2006), [arXiv:hep-ph/0601084 \[hep-ph\]](#), doi:10.1088/1126-6708/2006/01/164.
 60. W. Buchmuller, P. Di Bari and M. Plumacher, *New J. Phys.* **6**, 105 (2004), [arXiv:hep-ph/0406014 \[hep-ph\]](#), doi:10.1088/1367-2630/6/1/105.
 61. T. Frossard, M. Garny, A. Hohenegger, A. Kartavtsev and D. Mitrouskas, *Phys. Rev.* **D87**, 085009 (2013), [arXiv:1211.2140 \[hep-ph\]](#), doi:10.1103/PhysRevD.87.085009.
 62. M. Borah, D. Borah and M. K. Das, *Phys. Rev.* **D91**, 113008 (2015), [arXiv:1503.03431 \[hep-ph\]](#), doi:10.1103/PhysRevD.91.113008.
 63. R. Kalita, D. Borah and M. K. Das, *Nucl. Phys.* **B894**, 307 (2015), [arXiv:1412.8333 \[hep-ph\]](#), doi:10.1016/j.nuclphysb.2015.03.007.
 64. D. Borah and M. K. Das, *Phys. Rev.* **D90**, 015006 (2014), [arXiv:1303.1758 \[hep-ph\]](#), doi:10.1103/PhysRevD.90.015006.
 65. H. Zhang, *Phys. Lett.* **B714**, 262 (2012), [arXiv:1110.6838 \[hep-ph\]](#), doi:10.1016/j.physletb.2012.06.074.
 66. P. Das, A. Mukherjee and M. K. Das, *Nucl. Phys.* **B941**, 755 (2019), [arXiv:1805.09231 \[hep-ph\]](#), doi:10.1016/j.nuclphysb.2019.02.024.
 67. KATRIN Collaboration (A. Osipowicz *et al.*) (2001), [arXiv:hep-ex/0109033 \[hep-ex\]](#).
 68. S. Mertens, T. Lasserre, S. Groh, G. Drexlin, F. Glueck, A. Huber, A. W. P. Poon, M. Steidl, N. Steinbrink and C. Weinheimer, *JCAP* **1502**, 020 (2015), [arXiv:1409.0920 \[physics.ins-det\]](#), doi:10.1088/1475-7516/2015/02/020.
 69. R. E. Shrock, *Phys. Lett.* **96B**, 159 (1980), doi:10.1016/0370-2693(80)90235-X.
 70. A. Boyarsky, O. Ruchayskiy and M. Shaposhnikov, *Ann. Rev. Nucl. Part. Sci.* **59**, 191 (2009), [arXiv:0901.0011 \[hep-ph\]](#), doi:10.1146/annurev.nucl.010909.083654.
 71. C. Benso, V. Brdar, M. Lindner and W. Rodejohann, *Phys. Rev.* **D100**, 115035 (2019), [arXiv:1911.00328 \[hep-ph\]](#), doi:10.1103/PhysRevD.100.115035.
 72. E. Bulbul, M. Markevitch, A. Foster, R. K. Smith, M. Loewenstein and S. W. Randall, *The Astrophysical Journal* **789**, 13 (Jun 2014), doi:10.1088/0004-637x/789/1/13.
 73. A. Boyarsky, O. Ruchayskiy, D. Iakubovskiy and J. Franse, *Phys. Rev. Lett.* **113**, 251301 (Dec 2014), doi:10.1103/PhysRevLett.113.251301.
 74. A. Boyarsky, J. Franse, D. Iakubovskiy and O. Ruchayskiy, *Phys. Rev. Lett.* **115**, 161301 (2015), [arXiv:1408.2503 \[astro-ph.CO\]](#), doi:10.1103/PhysRevLett.115.161301.
 75. S. Riemer-Sørensen, *Astron. Astrophys.* **590**, A71 (2016), [arXiv:1405.7943 \[astro-ph.CO\]](#), doi:10.1051/0004-6361/201527278.
 76. F. Capozzi, E. Lisi, A. Marrone, D. Montanino and A. Palazzo, *Nucl. Phys.* **B908**, 218 (2016), [arXiv:1601.07777 \[hep-ph\]](#), doi:10.1016/j.nuclphysb.2016.02.016.
 77. G. Altarelli and F. Feruglio, *Nucl. Phys.* **B720**, 64 (2005), [arXiv:hep-ph/0504165 \[hep-ph\]](#), doi:10.1016/j.nuclphysb.2005.05.005.
 78. E. J. Chun, A. S. Joshipura and A. Yu. Smirnov, *Phys. Rev.* **D54**, 4654 (1996), [arXiv:hep-ph/9507371 \[hep-ph\]](#), doi:10.1103/PhysRevD.54.4654.
 79. K. S. Babu, TASI Lectures on Flavor Physics, in *Proceedings of Theoretical Advanced Study Institute in Elementary Particle Physics on The dawn of the LHC era (TASI 2008): Boulder, USA, June 2-27, 2008*, (2010), pp. 49–123. [arXiv:0910.2948 \[hep-ph\]](#).

80. R. Gonzalez Felipe, H. Serodio and J. P. Silva, *Phys. Rev.* **D88**, 015015 (2013), [arXiv:1304.3468 \[hep-ph\]](#), doi:10.1103/PhysRevD.88.015015.
81. N. Nath, M. Ghosh, S. Goswami and S. Gupta, *JHEP* **03**, 075 (2017), [arXiv:1610.09090 \[hep-ph\]](#), doi:10.1007/JHEP03(2017)075.
82. S. Weinberg, *Phys. Rev. Lett.* **43**, 1566 (Nov 1979), doi:10.1103/PhysRevLett.43.1566.
83. E. J. Chun, A. S. Joshipura and A. Yu. Smirnov, *Phys. Lett.* **B357**, 608 (1995), [arXiv:hep-ph/9505275 \[hep-ph\]](#), doi:10.1016/0370-2693(95)00967-P.
84. J. Heeck and H. Zhang, *JHEP* **05**, 164 (2013), [arXiv:1211.0538 \[hep-ph\]](#), doi:10.1007/JHEP05(2013)164.
85. C. Giganti, S. Lavignac and M. Zito, *Prog. Part. Nucl. Phys.* **98**, 1 (2018), [arXiv:1710.00715 \[hep-ex\]](#), doi:10.1016/j.pnpnp.2017.10.001.
86. S. Antusch, C. Biggio, E. Fernandez-Martinez, M. B. Gavela and J. Lopez-Pavon, *JHEP* **10**, 084 (2006), [arXiv:hep-ph/0607020 \[hep-ph\]](#), doi:10.1088/1126-6708/2006/10/084.
87. E. Akhmedov, A. Kartavtsev, M. Lindner, L. Michaels and J. Smirnov, *JHEP* **05**, 081 (2013), [arXiv:1302.1872 \[hep-ph\]](#), doi:10.1007/JHEP05(2013)081.
88. Z.-z. Xing (2019), [arXiv:1909.09610 \[hep-ph\]](#).
89. N. Gautam and M. K. Das (2019), [arXiv:1904.10662 \[hep-ph\]](#).
90. KamLAND-Zen Collaboration (S. Obara), *Nucl. Instrum. Meth.* **A845**, 410 (2017), doi:10.1016/j.nima.2016.06.059.
91. CUORE Collaboration (D. R. Artusa *et al.*), *Adv. High Energy Phys.* **2015**, 879871 (2015), [arXiv:1402.6072 \[physics.ins-det\]](#), doi:10.1155/2015/879871.
92. SNO+ Collaboration (J. Hartnell), *J. Phys. Conf. Ser.* **375**, 042015 (2012), [arXiv:1201.6169 \[physics.ins-det\]](#), doi:10.1088/1742-6596/375/1/042015.
93. NEXT Collaboration (J. J. Gomez-Cadenas *et al.*), *Adv. High Energy Phys.* **2014**, 907067 (2014), [arXiv:1307.3914 \[physics.ins-det\]](#), doi:10.1155/2014/907067.
94. A. S. Barabash, *J. Phys. Conf. Ser.* **375**, 042012 (2012), [arXiv:1112.1784 \[nucl-ex\]](#), doi:10.1088/1742-6596/375/1/042012.
95. KamLAND-Zen Collaboration (A. Gando *et al.*), *Phys. Rev. Lett.* **117**, 082503 (2016), [arXiv:1605.02889 \[hep-ex\]](#), doi:10.1103/PhysRevLett.117.082503, 10.1103/PhysRevLett.117.109903, [Addendum: *Phys. Rev. Lett.* 117, no. 10, 109903 (2016)].
96. H. Bhang *et al.*, *J. Phys. Conf. Ser.* **375**, 042023 (2012), doi:10.1088/1742-6596/375/1/042023.
97. EXO-200 Collaboration, D. Tosi, The search for neutrino-less double-beta decay: summary of current experiments, in *Proceedings, 14th ICATPP Conference on Astroparticle, Particle, Space Physics and Detectors for Physics Applications (ICATPP 2013): Como, Italy, September 23-27, 2013*, (2014), pp. 304–314. [arXiv:1402.1170 \[nucl-ex\]](#).
98. nEXO Collaboration (C. Licciardi), *J. Phys. Conf. Ser.* **888**, 012237 (2017), doi:10.1088/1742-6596/888/1/012237.
99. A. Berlin and D. Hooper, *Phys. Rev.* **D95**, 075017 (2017), [arXiv:1610.03849 \[hep-ph\]](#), doi:10.1103/PhysRevD.95.075017.
100. M. Drewes *et al.*, *JCAP* **1701**, 025 (2017), [arXiv:1602.04816 \[hep-ph\]](#), doi:10.1088/1475-7516/2017/01/025.
101. T. Asaka, M. Laine and M. Shaposhnikov, *JHEP* **01**, 091 (2007), [arXiv:hep-ph/0612182 \[hep-ph\]](#), doi:10.1088/1126-6708/2007/01/091, 10.1007/JHEP02(2015)028, [Erratum: *JHEP* 02, 028 (2015)].
102. X.-D. Shi and G. M. Fuller, *Phys. Rev. Lett.* **82**, 2832 (1999),

- arXiv:astro-ph/9810076 [astro-ph], doi:10.1103/PhysRevLett.82.2832.
103. M. Laine and M. Shaposhnikov, *JCAP* **0806**, 031 (2008), arXiv:0804.4543 [hep-ph], doi:10.1088/1475-7516/2008/06/031.
 104. G. B. Gelmini, P. Lu and V. Takhistov (2019), arXiv:1911.03398 [hep-ph].
 105. C. Yche, N. Palanque-Delabrouille, J. Baur and H. du Mas des Bourboux, *JCAP* **1706**, 047 (2017), arXiv:1702.03314 [astro-ph.CO], doi:10.1088/1475-7516/2017/06/047.
 106. J. Baur, N. Palanque-Delabrouille, C. Yche, A. Boyarsky, O. Ruchayskiy, . Armengaud and J. Lesgourgues, *JCAP* **1712**, 013 (2017), arXiv:1706.03118 [astro-ph.CO], doi:10.1088/1475-7516/2017/12/013.
 107. B. W. Lee and R. E. Shrock, *Phys. Rev. D* **16**, 1444 (Sep 1977), doi:10.1103/PhysRevD.16.1444.
 108. P. B. Pal and L. Wolfenstein, *Phys. Rev. D* **25**, 766 (Feb 1982), doi:10.1103/PhysRevD.25.766.
 109. A. Abada, G. Arcadi and M. Lucente, *JCAP* **1410**, 001 (2014), arXiv:1406.6556 [hep-ph], doi:10.1088/1475-7516/2014/10/001.
 110. K. C. Y. Ng, B. M. Roach, K. Perez, J. F. Beacom, S. Horiuchi, R. Krivonos and D. R. Wik, *Phys. Rev. D* **99**, 083005 (2019), arXiv:1901.01262 [astro-ph.HE], doi:10.1103/PhysRevD.99.083005.
 111. A. D. Linde, *Phys. Lett.* **70B**, 306 (1977), doi:10.1016/0370-2693(77)90664-5.
 112. C. G. Callan, Jr., R. F. Dashen and D. J. Gross, *Phys. Lett.* **B63**, 334 (1976), doi:10.1016/0370-2693(76)90277-X, [,357(1976)].
 113. F. R. Klinkhamer and N. S. Manton, *Phys. Rev. D* **30**, 2212 (1984), doi:10.1103/PhysRevD.30.2212.
 114. A. S. Joshipura, E. A. Paschos and W. Rodejohann, *Nucl. Phys. B* **611**, 227 (2001), arXiv:hep-ph/0104228, doi:10.1016/S0550-3213(01)00346-7.
 115. A. Abada, C. Biggio, F. Bonnet, M. B. Gavela and T. Hambye, *JHEP* **12**, 061 (2007), arXiv:0707.4058 [hep-ph], doi:10.1088/1126-6708/2007/12/061.
 116. A. Ibarra, E. Molinaro and S. T. Petcov, *JHEP* **09**, 108 (2010), arXiv:1007.2378 [hep-ph], doi:10.1007/JHEP09(2010)108.
 117. A. Das and N. Okada, *Phys. Lett.* **B774**, 32 (2017), arXiv:1702.04668 [hep-ph], doi:10.1016/j.physletb.2017.09.042.
 118. M. Viel, J. Lesgourgues, M. G. Haehnelt, S. Matarrese and A. Riotto, *Phys. Rev. Lett.* **97**, 071301 (2006), arXiv:astro-ph/0605706 [astro-ph], doi:10.1103/PhysRevLett.97.071301.
 119. U. Seljak, A. Makarov, P. McDonald and H. Trac, *Phys. Rev. Lett.* **97**, 191303 (2006), arXiv:astro-ph/0602430 [astro-ph], doi:10.1103/PhysRevLett.97.191303.
 120. M. Viel, G. D. Becker, J. S. Bolton and M. G. Haehnelt, *Phys. Rev. D* **88**, 043502 (2013), arXiv:1306.2314 [astro-ph.CO], doi:10.1103/PhysRevD.88.043502.
 121. C. Schultz, J. Oorbe, K. N. Abazajian and J. S. Bullock, *Mon. Not. Roy. Astron. Soc.* **442**, 1597 (2014), arXiv:1401.3769 [astro-ph.CO], doi:10.1093/mnras/stu976.